Available online at www.sciencedirect.com
SCIENCE DIRECT®
Journal of Molecular Graphics and Modelling 23 (2004) 263–273
Journal of Molecular Graphics and Modelling
www.elsevier.com/locate/JMGM

Modeling the α-helix to β-hairpin transition mechanism and the formation of oligomeric aggregates of the fibrillogenic peptide Aβ(12–28): insights from all-atom molecular dynamics simulations

Fabio Simona[a,b], Guido Tiana[b,c], Ricardo A. Broglia[b,c,d], Giorgio Colombo[a,*]

[a]*Istituto di Chimica del Riconoscimento Molecolare, CNR, Via Mario Bianco 9, 20131 Milano, Italy*
[b]*Dipartimento di Fisica, Università di Milano, Via Celoria 16, I-20133 Milano, Italy*
[c]*INFN, Sezione di Milano, Via Celoria 16, I-20133 Milano, Italy*
[d]*Niels Bohr Institute, Bledgamsvej 17, 2100 Copenhagen, Denmark*

Received 14 April 2004; received in revised form 26 July 2004; accepted 26 July 2004

Abstract

In this paper, all-atom molecular dynamics simulations in explicit solvent are used to investigate the structural and dynamical determinants of the α-helical to β-hairpin conformational transition of the 12–28 fragment from the full length Aβ Alzheimer's peptide. The transition from α-helical to β-structure requires the peptide to populate intermediate β-bend geometries in which several mainly hydrophobic interactions are partially formed. This is followed by the sudden collapse to ordered β-hairpin structures and the simultaneous disruption of the hydrophobic side-chain interactions with a consequent increase in solvent exposure.

The solvent exposure of hydrophobic side-chains belonging to a sequence of five consecutive residues in the β-hairpin defines a possible starting point for the onset of the aggregation mechanisms. Several different conformations of model oligomeric (dimeric and tetrameric) aggregates are then investigated. These simulations show that while hydrophobic contacts are important to bring together different monomers with a β-hairpin like conformation, more specific interactions such as hydrogen-bonding and coulombic interactions, should be considered necessary to provide further stabilization and ordering to the nascent fibrillar aggregates.

Keywords: Protein misfolding; Aggregation models; Molecular dynamics; Fibril formation

1. Introduction

Peptide and protein misfolding to non-native forms underlies a wide number of degenerative diseases in humans, generally defined amyloidoses. Misfolded species in the cell are in general subject to control mechanisms that lead to their degradation. In many cases, however, they self-assemble and form insoluble supramolecular species known as amyloid fibrils. Amyloid fibrils are filamentous aggregates, typically 0.1 to 10 μm long and about 10 nm wide. Current focus on fibril formation and aggregation phenomena stems from their association with amyloid diseases. These include Alzheimer's disease, type 2 diabetes, prion disease, Parkinson's disease, senile systemic amyloidosis and Huntington's disease. As a consequence, understanding the biochemical and biophysical reasons that cause soluble peptides and proteins to undergo conformational changes from the native conformation to disease-inducing ones, and obtaining an atomically detailed picture of the structures of the aggregates represents a major interest both from the practical and the theoretical points of view.

In amyloidoses, the soluble native state N of the peptide or protein undergoes a conformational change and starts assembling into an amyloid fibril [1]. Lansbury and co-workers [2] showed that in Alzheimer's disease the amyloid assembly process is modular, with at least two quaternary structural intermediates (protofilaments) combining during amyloid filament assembly. However, other evidences

* Corresponding author. Tel.: +39 02 285 000 31; fax: +39 02 285 000 36.
E-mail address: giorgio.colombo@icrm.cnr.it (G. Colombo).

1093-3263/$ – see front matter © 2004 Elsevier Inc. All rights reserved.
doi:10.1016/j.jmgm.2004.07.004

showed that Alzheimer's amyloid can grow through the binding of monomers to the ends of the growing fibril. In contrast to Alzheimer's disease, the amyloidogenic intermediate of other amyloid disease proteins and peptides appear to be less structured.

From the experimental point of view [3–5] X-ray fiber diffraction and solid state NMR analysis have revealed that a common trait of amyloid fibrils is the presence of the cross-β structural motif, in which ribbon-like β-sheets, extending over the length of the fibril, are formed by β-strands that run perpendicular to the long axis of the fibril, with backbone hydrogen bonds parallel to the axis. Apart from the extensive presence of the β-motif, little is known about the molecular structure of amyloid fibrils. Moreover, little is known about the mechanism driving an otherwise soluble peptide to populate conformations leading to aggregation and to the formation of insoluble fibrils [6].

Despite the enormous progress achieved by experimental approaches, especially in the fields of X-ray and NMR, to obtain a clear atomistic picture both of the mechanism leading to the appearance of the aggregating monomer and of the factors determining the stability of protofibrils, one has little choice but to turn to theoretical methods.

A great deal of attention in recent literature has been devoted to the study peptide Aβ(1–42), responsible for the deposition in human brains of plaques causing Alzheimer's disease, and fragmentes of Aβ(1–42) which retain the ability of forming fibrils like Aβ(12–28). Molecular dynamics (MD) simulations have been used to investigate the molecular properties of selected fragments. Klimov and Thirumalai [7] showed through MD that the oligomerization of Aβ(16–22) requires the peptide to undergo a random coil to α-helix to β-strand transition. Straub et. al used the computation of a variationally optimized dynamical trajectory connecting fixed end points of known structure to speed up the conformational transitions among the different secondary structure motifs [8]. On the aggregation side, Caflish and co-workers used a simplified implicit solvent model to simulate the aggregation process of the heptapeptide GNNQQNY from the yeast prion protein [9]. Other MD simulations with explicit representations of the solvent were run on oligomers of the Alzheimer's peptides and the results indicate that A β(16–22) aggregates forming antiparallel β-sheets, and that longer fragments tend to form aggregates of β-hairpins [10]. These studies however do not consider the dynamic mechanism leading to the formation of the β-hairpins or their possible different ways of packing into ordered protofibrils.

In this paper, we report the results of all-atom molecular dynamics (MD) simulations of the conformational evolution of fragment Aβ(12–28) from Alzheimer's peptide (see Fig. 1). Several shorter synthetic fragments of the Aβ-peptide (1–28, 25–35, 10–35 and 12–28) have been studied and characterized. The peptide chosen for this study A β(12–28), in particular, was shown to have behavioral effects in mice [11,12], formation of fibril aggregates [13] and toxic effects

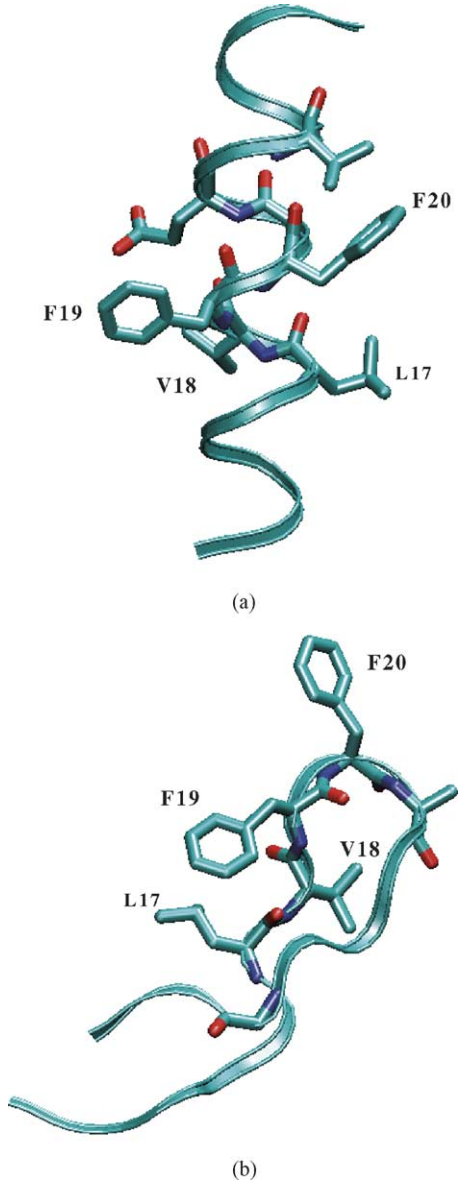

Fig. 1. The helical starting conformation (a) and the bent starting conformation obtained by structural clustering (b) (side-chains are explicitly shown).

in vitro [14]. In 2,2,2-trifluoroethanol (TFE) or membrane mimicking environments the Aβ(12-28) fragment was shown to adopt an α-helical conformation [15]. Several simulations were run for the monomeric Aβ(12–28) and oligomeric assemblies of the peptide in explicit water. Different starting structures and temperature conditions were used for the MD study of the monomer, with the aim of increasing conformational sampling. In the case of the oligomeric complexes, several different arrangements were tested for their overall dynamical behavior in the time scales accessible to all-atom molecular dynamics. The dimers and tetramers were built based on the final equilibrated conformation obtained from the monomer simulations, with different relative orientations of the constituent monomers. In particular several different juxtapositions of the planes of

β-hairpins were examined: in the dimer simulations the two planes were parallel ($2P_2$), antiparallel (2C) or with the hydophobic cores of the hairpins facing each other (2FH). In the tetramer simulations four parallel planes ($4P_4$) or an X-shaped arrangement of the hairpins with the hydrophobic cores directed towards the center of a hypothethical micelle (4S). This strategy based on the construction of defined dimeric or tetrameric geometries (see Table 1) should provide information on the physico–chemical factors responsible for protofibril stabilization.

2. Material and methods

Molecular dynamics simulations of monomers were run using different starting conformations at two different temperatures (295 and 320 K). The initial structures for the two simulations (100 ns each) of monomers starting from the helical conformation were obtained from the NMR-structure of the A β(1–28) peptide (pdb code 1AMB.pdb), by cutting the N-terminal 1 to 11 residues using the swisspdbviewer package [16]. Two more simulations (30 ns each) were run starting from a completely extended conformation for the monomeric peptide, obtained by imposing an all-trans geometry to every backbone dihedral. Finally, two monomer simulations (100 ns) were started from a bent conformation of the A β(12–28) peptide, obtained by the structural clustering of the total ensemble of conformations spanned in the previous four simulations. The terminal residues of the peptide are considered uncharged.

The final equilibrated β-hairpin structure obtained at the end of the previous simulation was used to build models of several possible oligomeric aggregates. All the production runs of the oligomeric assemblies were 30 ns long.

Table 1 summarizes the details of the simulations—the temperature, the length and the labels which were assigned to each simulation.

Table 1
Simulation labels, conditions and time length

Starting structures	Number of water molecules	Simulated time (ns)
Monomers		
Helical (295 and 320 K)	2463	100
Fully extended (295 K)	11712	30
Fully extended (320 K)	11712	22
β-bend (295 and 320 K)	3757	100
Dimers at 300 K		
$2P_2$_far	3918	27.5
$2P_2$_near	2827	30
2FH	8202	30
2C	2753	30
Tetramers at 300 K		
4S	10597	30
$4P_4$	8341	30

The peptides and the complexes were solvated with water in a periodic truncated octahedron, large enough to contain the peptide and 0.9 nm of solvent on all sides. All solvent molecules within 0.15 nm of any peptide atom were removed. No counter-ions were added as water is a high dielectric and the inclusion of no counter-ions was considered a better approximation to the low salt experimental conditions. The resulting systems was composed of the complex and about three thousand water molecules. The details of the setup of the simulations are reported in Table 1.

The system was subsequently energy minimized with a steepest descent method for 1000 steps. In all simulations the temperature were maintained close to the intended value of 300 K by weak coupling to an external temperature bath [17] with a coupling constant of 0.1 ps. The complexes and the rest of the system were coupled separately to the temperature bath. The GROMOS96 force field [18,19] with the simple point charge (SPC) [20] water model was used. The LINCS algorithm [21] was used to constrain all bond lengths in the solute and the SETTLE algorithm [22] was used for water molecules. A dielectric permittivity, $\varepsilon = 1$, and a time step of 2 fs were used. The calculation of electrostatic forces utilized the PME implementation of the Ewald summation method [23]. Lennard–Jones interactions were calculated within a cut-off radius of 0.9 nm.

All atoms were given an initial velocity obtained from a Maxwellian distribution at the desired initial temperature. The system density was adjusted performing the first equilibration runs at NPT condition by weak coupling to a bath of constant pressure ($P_0 = 1$ bar, coupling time $\tau_P = 0.5$ ps) [17]. All the simulations, starting from the appropriate complex geometry, were equilibrated by 50 ps of MD runs with position restraints on the peptide to allow relaxation of the solvent molecules. These first equilibration runs were followed by other 50 ps runs without position restraints on the peptide. The production runs using NVT conditions, after equilibration, were 50 ns long for all ten complexes.

All the MD runs and the analysis of the trajectories were performed using the GROMACS software package [24].

3. Results and discussion

The principal goal of MD simulations is to obtain a dynamical picture of the events taking place in solution regarding both the monomers and the modeled oligomeric complexes. In the case of the monomers, the aim is to identify the conformational changes leading to the formation of ordered β-structure identified as a fibril constituent by experimental observations. The conformations obtained from the analysis of monomeric trajectories are then used to model the possible structures of oligomeric complexes. Given the complexity and the time scales of amyloid fibrillization, all-atom MD simulations of the whole process are not accessible or viable at the moment. The aim of the

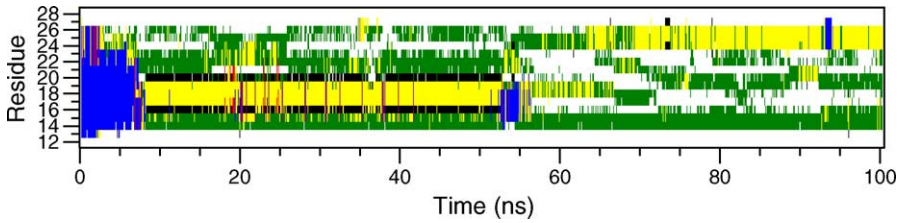

Fig. 2. Secondary structure time evolution of Aβ(12–28) starting from the helical geometry at 320 K.

oligomeric complex simulations is, on the one hand, to discriminate the relative stability of possible aggregation seeds in analogous conditions, and on the other hand to yield atomically detailed information on the intermolecular interactions responsible for stabilizing particular complexes.

3.1. The Monomers

3.1.1. Helical starting structures

The first two 100 ns long simulations of Aβ(12–28) were started from the helical conformation characteristic of the Aβ(1–28) fragment in the full length Aβ(1–42) peptide and in TFE solution.

The helical conformation was not stable and was lost after 20 ns at 295 K and 8 ns at 320 K; in each case, the first element to unfold is region 23–27 (Fig. 2). At the latter temperature, the unfolding of the helical structure starts from the C-terminus and involves mainly residues 22–28. The peptide shows a high tendency to populate an ensemble of bent conformations stabilized by the formation of a salt–bridge between K16 and E22 or D23, and by the packing of the side-chains of residues 17–21 (LVFFA), the central hydrophobic core (CHC), which tend to assume a turn-like conformation. The packing of V24 on the CHC and the presence of a stable hydrogen bond between LEU16 and PHE20, impart further stability to this nascent hydrophobic patch.

This conformation, while favoring the reduction of hydrophobic contact with the solvent with respect to the initial helical structure (CHC solvent accessible surface area is 5.8 nm^2 in the hairpin conformation versus 8 nm^2 in the helical conformation), determines an arrangement of five consecutive hydrophobic residues on one plane that can act as a possible hook to bind other monomers in analogous conformations. In the helical arrangement, these residues, while being exposed, point into different directions in space due to the structural requirements imposed by the helical geometry (Fig. 1(a)). The analysis of the internal energy profile of Aβ(12–28) shows first an increase in energy linked to the breaking of helical stabilizing hydrogen bonds, followed by a significant decrease during the formation of the compact bent structure.

A qualitatively similar behavior emerges also from the analysis of the trajectory at 295 K, where despite the unfolding of the helical structure being slower, a turn-like conformation in CHC is achieved, this time stabilized by a salt–bridge between LEU16 and GLU22, and an hydrogen bond (GLN15–PHE19). Conformational reversibility to the initial α-helix is not observed on the time scale examined, and would in any case require a much longer sampling of the conformational evolution, which is out of the scope of this paper.

3.1.2. Fully extended starting structures

Two more simulations for the monomer in water were started from fully extended conformations to increase conformational sampling. In these simulations the number of solvating water molecules increases by about one order of magnitude due to the dimensions of the periodic box, forcing the simulations to be carried out on shorter (30 ns) time scales.

An evident compaction of the system is observed at both temperatures, with the formation of a compact conformation of the peptide, characterized by the presence of a loop comprising residues 20–24, and by the packing of VAL24 on CHC (see Fig. 3). The limited time span of the simulations prevents the observation of the formation of structures with a higher order degree, however they can show that the peptide tends to populate an ensemble of bent conformations analogous to those found in the previous simulations starting from helical geometries.

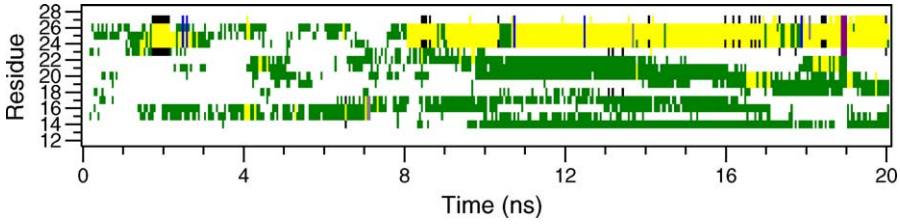

Fig. 3. Secondary structure time evolution of Aβ(12–28) starting from totally extended geometry at 320 K.

3.1.3. β-Bent starting structure

Considering the tendency of the peptide to fall into a bent conformation with a turn-like region exposing the side-chains of CHC residues, a clustering procedure [25] was run on all the structures obtained from the combination of the four trajectories discussed above. Cluster analysis was performed using the Jarvis and Patrick [25] method—a structure is added to a cluster when this structure and a structure in the cluster have each other as neighbors and they have at least P neighbors in common. The neighbors of a structure are the M closest structures or all the structures within a cut-off. In our case P is 3, M is 9 and the cutoff value is 0.1 nm. As expected the representative structure of the most populated cluster displays a loop involving residues 20–24 (see Fig. 1(b)). This representative structure was thus isolated and used as a starting point for two more MD simulations of 100 ns. At the lower temperature the peptide maintains the loop conformation for residues 20–24, and jumps between different energetically close minima, without reaching a stable dominant state. Interestingly, ordered β-hairpin structures appear during the simulation. Increasing the temperature to 320 K allows the peptide to escape the local minimum trapping it in the bent conformation. After ≈48 ns a sharp transition to a very ordered β-hairpin structure is observed (Fig. 4). The β-hairpin structure was of the type 2:2 with a type II' β-turn sequence of F19-F20-A21-E22. Very interestingly, the hydrophobic side chains of LVFFA sequence, as a consequence of both being consecutive in the sequence and of the formation of the turn, were mostly exposed to water. This conformation is stabilized by salt–bridges between VAL12–LYSH28 and LYSH17–ASP23 and hydrogens bonds (LEU17–VAL24, GLN15–SER26, HIS13–LYSH28 and LEU17–SER26. Only in helical conformations was it possible to find such a high number of local stabilizing interactions, and the average internal energies for the two conformations turned out to be rather similar: −887 kJ/mol for the α-helics and −881 kJ/mol for the β-hairpin.

An important feature in the β-hairpin conformation is represented by the stereochemical arrangement and spatial disposition of the hydrophobic side-chains belonging to CHC. These side chains are all consecutive in sequence and have a very ordered space directionality, due to the homochiral constraints imposed by constituting aminoacids. This feature defines a very ordered interaction area, with the structural preorganization properties necessary to induce ordered docking of other similar monomers.

4. Oligomers

The structural features and the stability of the β-hairpin conformation, combined with the experimental observations suggesting a high percentage of β-structure in amyloid fibrils, lead to the choice of the β-hairpin as the monomeric unit on which model oligomeric complexes could be built. All-atom simulations in explicit solvent on the oligomers were all 30 ns long.

4.1. Dimers

Three different starting structures were used to model a dimeric complex, with two chains labeled respectively A and B. (1) *The parallel planes conformations* (Fig. 5(a)) (simulation labeled $2P_2$): the starting structure is built such that the planes defining the β-hairpin are parallel, with the CHC regions directly facing each other, in a way that should favor possible hydrophobic type interactions. (2) *Facing hydrophobic patches*, labelled 2FH: the CHC regions of each monomer are on the same plane, and directly face each other (Fig. 5(b)). (3) *Parallel planes, opposite directions* (label 2C): the hairpins are on parallel planes, with the CHC region of one monomer facing the termini of the hairpin of the other (Fig. 5(c)).

4.1.1. Simulation $2P_2$

The starting structure in simulation $2P_2$was designed such that possible intermolecular hydrophobic interactions could be localized mainly in the facing CHC-loop regions, while electrostatic and hydrogen-bonding interactions could be mainly located in the strands of the β-hairpins.

Two different peptide center of mass (COM) distances were used in these simulations. In the first one, the two COM were set to 1.5 nm. This distance value decreases to about 1.2 nm in the course of the simulation (Fig. 6 $2P_2$_near) to increase to 1.6 nm in the final stages. The COM distance of the two CHC regions, parallels this evolution. The intermolecular contacts formed in this simulation are mainly two hydrogen bonds involving GLY25 on chain A and LYS16 on chain B plus ASN27A and HIS13B. Two more hydrogen-bonding interactions can form around 20 ns, one

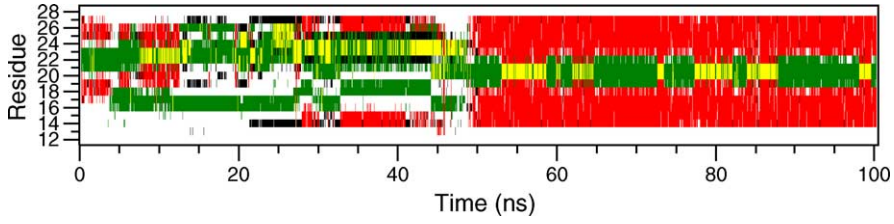

Fig. 4. Secondary structure time evolution of A β(12–28) starting from the bent conformation at 320 K.

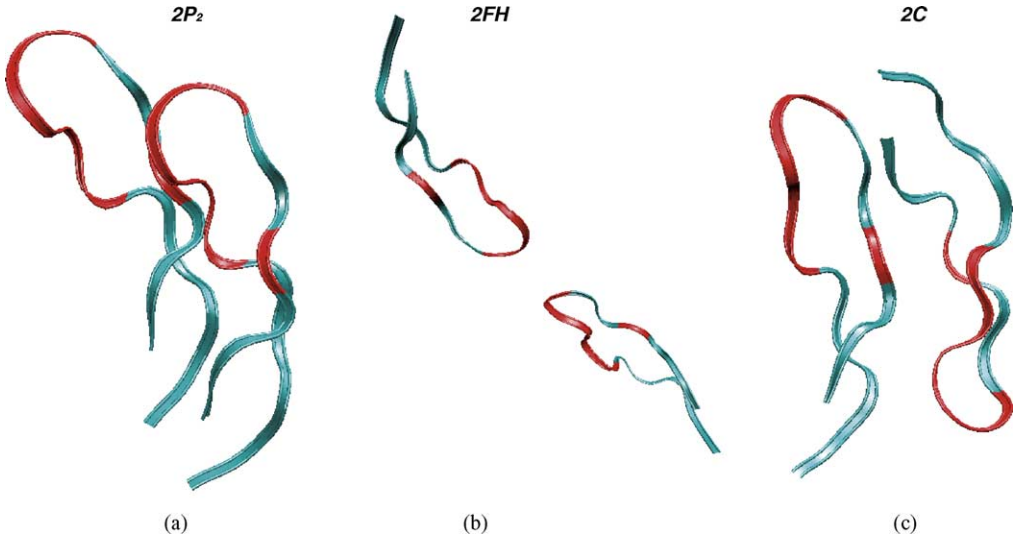

Fig. 5. Starting arrangements of dimer simulations. The red bands indicate the positions of hydrophobic residues.

involving HIS13A and HIS13B and the other involving GLY25A and LYS16B.

Evolution of the number of hydrogen-bonding interactions is reported in Fig. 7. In the second simulation, the two CHC regions are put directly in contact by imposing a COM distance for CHC of 0.8 nm. In this case as well, ordering intermolecular hydrogen-bonding interactions form between parallel strands. The most stable ones are between ASN27A and SER26B, formed reversibly during the simulation and between ASN27A and ASN27B. ASN27B is moreover involved in stable hydrogen bonds with SER26 of monomer A. During the course of the simulation, the distance between the two CHC increases from about 0.8 nm to about 0.9 nm. It is worth noting, that neither in the first simulation of the $2P_2$arrangement, nor in the second, is there

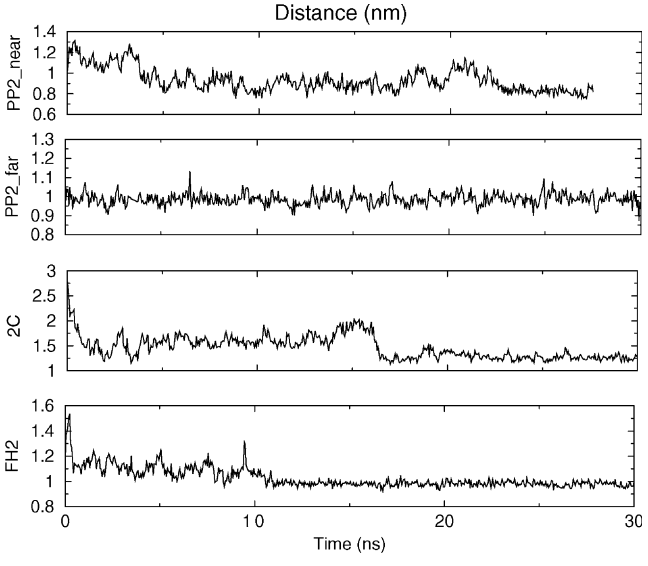

Fig. 6. Time evolution of the center of mass (COM) distances of the four dimers simulations.

a noticeable decrease in the solvent accessible surface (SAS) area of the CHC regions. The result of these two simulations point to the fact that, while hiding hydrophobic residues of CHC from an unfavorable contact with water can be important in gluing the two monomers together, structural ordering in the dimer is obtained mainly by other types of interactions, namely hydrogen-bonding ones.

4.1.2. Simulation 2FH

To investigate the role of hydrophobic forces in the stabilization of the dimer, the 2FH arrangement shown in (Fig. 5(b) was designed and its time-evolution was investigated. The only contact point between the two monomers is represented by the CHC regions. The analysis of the time evolution of the COM distances for the whole peptides and of the CHC indicates a significant decrease at about 18 ns, paralleled by a significant decrease in the value of Lennard–Jones interaction energy. In this case, the two peptides reorganize their respective orientations, towards a structural situation with parallel planes between the two β-hairpins. The CHC regions act as hinges modulating the motion of the peptides. Hydrogen bond ordering and more specific interactions than just the hydrophobic ones formed between VAL18A and PHE20B, PHE20A and GLN15B, PHE20A and LYS16B. As the time evolution increases, the two peptides increase their tendency to pack with hairpin parallel planes on top of each other in such a way as to maximize hydrogen-bonding and electrostatic intermolecular interactions.

4.1.3. Simulation 2C

To test the role of electrostatic and hydrogen-bonding interactions in determining an ordered supramolecular organization, arrangement 2C was tested (see Fig. 5(c)), and the starting distance between the COM of parallel planes was set to 1.2 nm. In this starting conformation, the CHCs

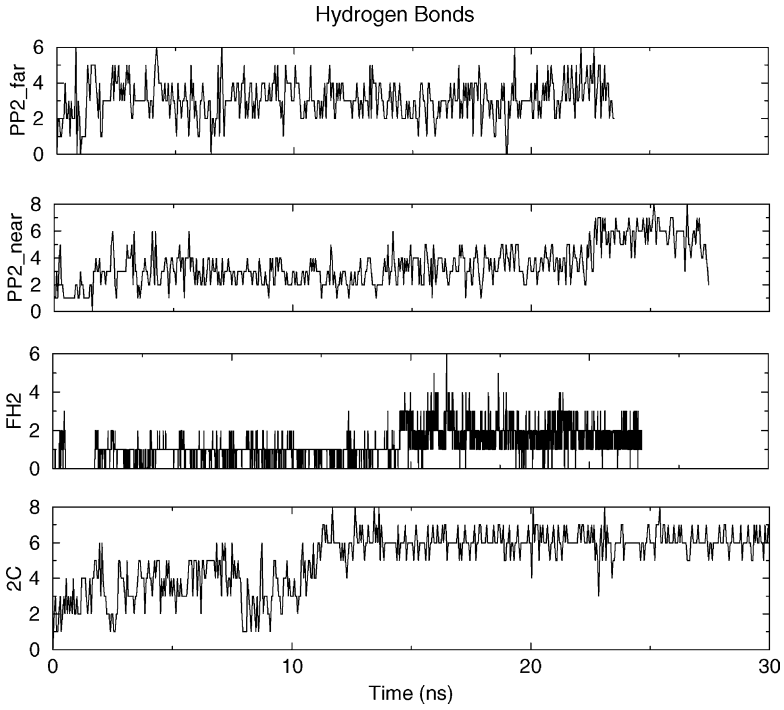

Fig. 7. Number of hydrogens bond in function of time in dimers simulations.

point into opposite directions and their contacting interactions are minimized. The starting configuration is stable throughout the whole simulation time range. Moreover, after about 10 ns of equilibration a dramatic decrease in the internal energy value is noticed, corresponding to the onset of several intermolecular H-bonding interactions, besides the ones present at the beginning of the simulation (SER26A with GLU22B, and ASN27A with GLU22 B). The newly formed interactions involve GLU22A and SER26B plus GLU22A and ASN27B.

In all of the simulations described above, the secondary structure content does not change with time and the β-hairpin secondary structure is well conserved throughout the simulations.

4.2. Tetramers

The results of the above reported simulations suggest an interplay between the role of hydrophobic interactions involving CHC residues and the role of hydrogen bond and electrostatic interactions involving residues of the strands. In particular, the role of CHC seems to be that of bringing peptides together, while that of intermolecular H-bonding and electrostatic interactions is to bring about some further degree of ordering.

These factors were further investigated in tetrameric aggregates, which can be considered a nascent protofibrils. Three different starting conformations, each obtained by the juxtaposition of two replicas of each of the dimeric arrangements described above, were run and analyzed. The combination of two dimers of the 2C type resulted in a fast disassembly of the starting tetrameric structure into two isolated dimers, and will not be discussed further.

In the remaining two trajectories the four monomers were arranged in 4 parallel planes with the CHC regions pointing into the same direction, and in a plane with the four CHC regions pointing to the center of an ideal circle with the charged strands pointing outside as in the possible nascent state of a micellar aggregate. The two simulations are labeled 4 parallel planes ($4P_4$) and 4 star (4S) (see Fig. 8a and b), respectively.

4.2.1. Simulation $4P_4$

The analysis of the 30 ns long MD trajectory of the tetramer represented in Fig. 8(a) was performed with the main goal of understanding whether the same stabilizing motifs present in the dimer are present in higher order aggregates. In other words, this analysis should clarify whether the presence of four consecutive CHC regions can provide significant hydrophobic packing stabilization, and how intermolecular electrostatic and hydrogen-bonding interactions participate to the structural ordering of this fibril building block.

From the structural point of view the packing between CHC regions is particularly tight only between chains A and B, with a COM distance for the CHC region of about 0.75 nm, while in the case of chains B–C and C–D the packing is not optimal (0.9 nm), even though hydrophobic contacts are still present. The supramolecular aggregate is stabilized by a network of interchain hydrogen-bonding interactions (Fig. 9). Particularly stable contacts between chains A and B are: GLN15A–ASN27B, HIS14A–PHE19B,

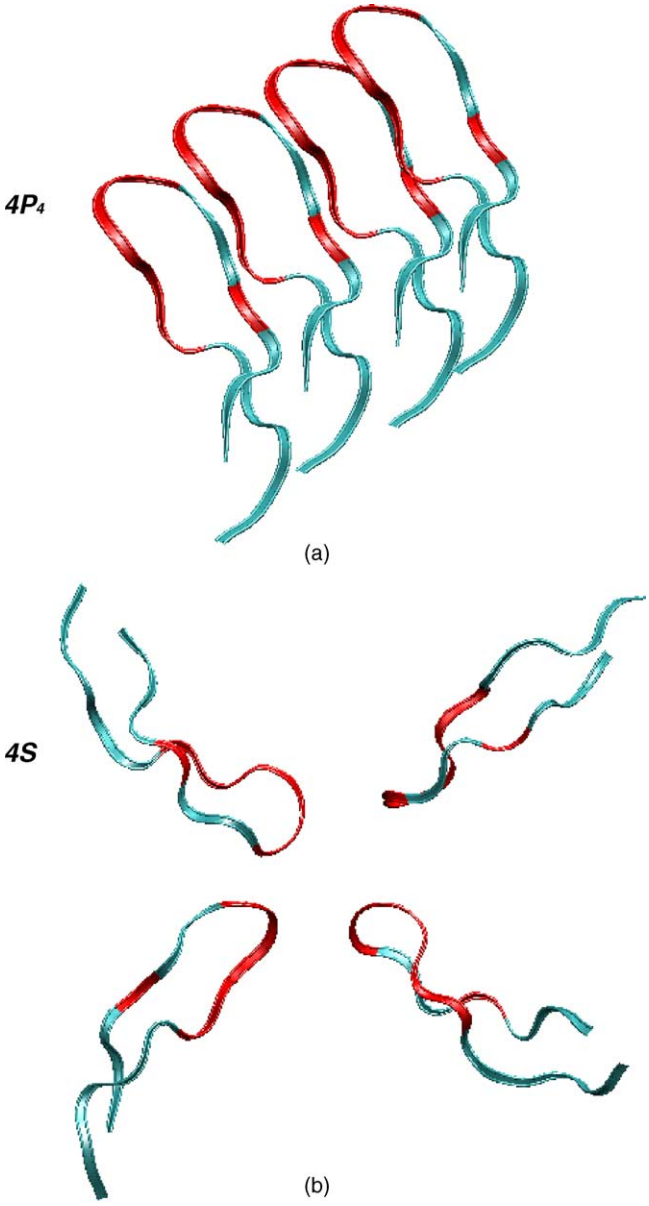

Fig. 8. Starting arrangements of tetramer simulations. The red bands indicate the positions of hydrophobic residues.

VAL18A–GLN15B, and VAL24A–LYS16B. Chains B and C are also stabilized by a series of hydrogen bonds, in particular, GLY25B–HIS13C, SER26B–VAL12C, ASN27B–VAL12C or ASN27C and HIS14B–HIS14C. No particularly persistent interaction is observed between chains C and D, and this factor drives the system to a situation of low stability where the initial tetrameric arrangement is disrupted over the simulation time. Analysis of the CHC solvent accessible area shows how the water contact area tends to decrease during the simulation time (Fig. 10).

4.2.2. Simulation 4S

The X-shaped starting structure, was used to investigate whether the formation of a stable hydrophobic core, protected from the solvent by its burial by means of the hydrophilic groups in the strands, is stable enough (in MD simulations) to be considered the seed for the formation of possible transient micellar states (Fig. 8(b)).

Inspection of MD simulations shows that the 4S (X-shaped) conformation is rapidly lost. In particular, the constituting peptides tend to move from their starting positions to a final conformation where the CHC regions are superimposed and where the strands of each monomer lie on parallel planes. This type of movement is the same as that observed in the dimer, and the stabilizing electrostatic and H–bonding interactions are fundamentally the same as those described in the dimer parallel plane situation. The $4P_4$ arrangement thus shows a tendency to form a structure which is globally similar to the $4P_4$ one (Fig. 11). This type of arrangement is consistent with a free energy minimum conformation calculated with a thermodynamical model developed to study fibril formation (see Tiana et al. in J. Chem. Phys. (2004) [26]) and with several theoretical and experimental hypotheses on how monomers must be organized in the fibril (Daidone, Proteins: Structure, Function and Bioinformatics, 2004, in press).

Taken together the results of our unbiased simulations on the conformational evolution of the monomer and on model aggregates can help shed light on the physico–chemical factors underlying the formation of small aggregates at the basis of amyloid fibril growth. In particular, we could show that the extreme conformational flexibility of the monomer, and its very peculiar sequence with five consecutive hydrophobic residues favor the formation of an ordered β-hairpin structure. This structure is characterized by the presence of a turn region comprising residues 20–24, part of the central hydrophobic core, which forces the hydrophobic side chains of those amino acids to define a continuous planar hydrophobic patch. This type of structure can be considered as highly frustrated and offers a clear starting point for aggregation—other monomers with the same properties can pack on top of each other, using the exposed hydrophobic patches as interaction points, leading the fibril to grow and eventually precipitate. The analysis of the simulations on dimeric and tetrameric aggregates show that hydrophobic interactions alone cannot impose the necessary structural restraints to form an ordered supramolecular aggregate. The ordered arrangement of the side-chains in CHC helps in defining the overall interaction stereochemistry among different monomer, but it is through the even more directional hydrogen-bonding and electrostatic (salt–bridges) interactions that oligomeric constructs can be stabilized in a non-random conformation.

Overall, these results show that the sequence of side-chains and their relative orientations play a decisive role in the formation of protofibrils. Not only do side chains have to interact through Van der Waals interactions, but they also have to interact in a stereochemically correct way; the amino

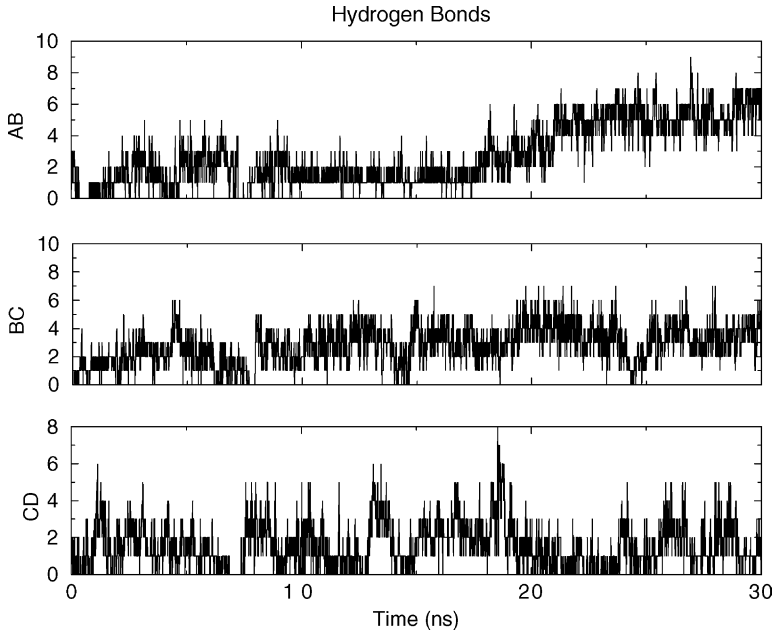

Fig. 9. Number of hydrogen bonds between adjacent monomers in $4P_4$ simulation.

acids in the strands of the peptides under study are all enantiopure L-enantiomers, so that the strands have to gain the proper directionality to maximize the number of stabilizing interstrand interactions. These aspects had already been noticed as fundamental in the investigation of models for the folding of closely related β-hairpin peptides.

Moreover, our models are in very good agreement with the well estabilished experimental evidences that amyloid fibrils are rich in β-sheet structure. In particular, in the case of Aβ-peptides, Serpell and co-workers, in their X-ray study of Alzheimer's related amyloid fibrils, have shown that β-hairpins have to be considered the conformation of the constitutive monomeric unit [27]. From the practical point of view, simulating minimal model peptides in explicit solvents such as the ones presented here can be a promising approach to complement experiments to solve the problem of rational control over macromolecular architecture. Our simple MD

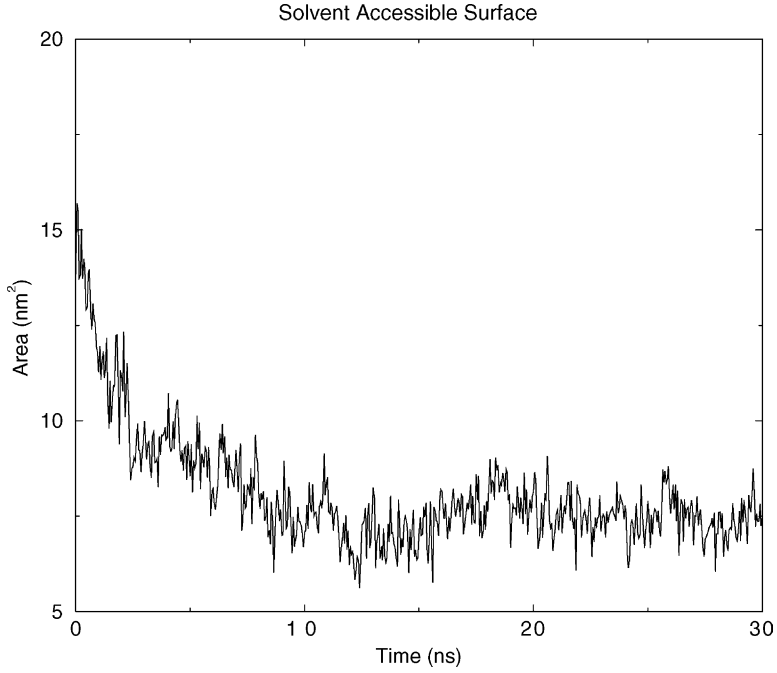

Fig. 10. Evolution of CHC solvent accessible area of $4P_4$ simulation.

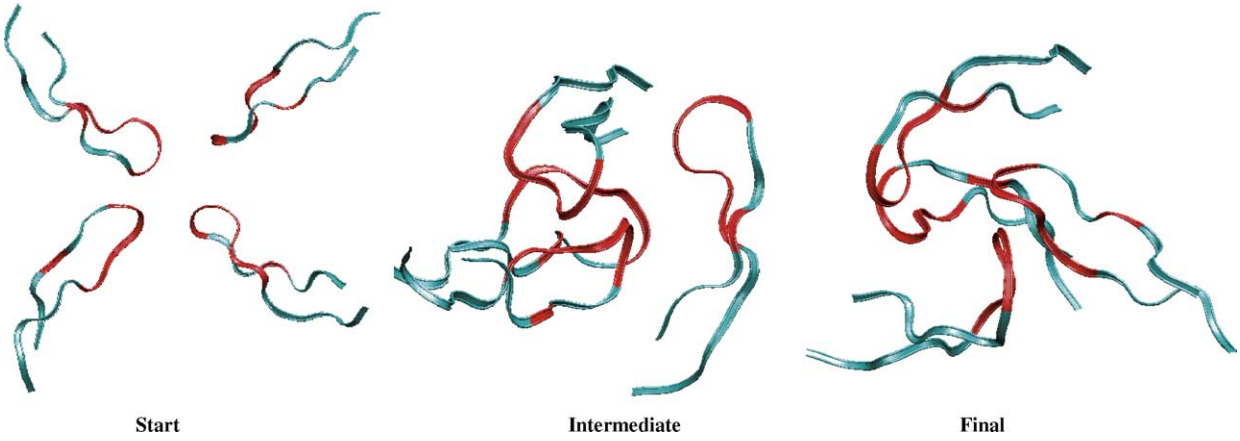

Fig. 11. Evolution of X-shaped structure towards a parallel plane arrangement.

simulations in fact proved able to catch the fine details and the main characterizing features of the systems under study. Theoretical studies like the ones presented here can pinpoint and allow control on a wide set of variables, such as sequence, stereochemistry, solvent conditions, with the final goal of rationally designing new polymers for material science or new leads for amyloid-breaking drug development.

5. Conclusions

In this paper, all-atom molecular dynamics simulations in explicit solvent were used to investigate the structural and dynamical determinants of the transition of the Aβ(12–28) peptide from a non-aggregating conformation to a possible amyloid forming one. The transition from α-helical to β-structure requires the peptide to populate intermediate β-bend geometries in which several mainly hydrophobic interactions are partially formed. This is followed by the sudden collapse to ordered β-hairpin structures and the simultaneous disruption of the hydrophobic side-chain interactions with a consequent increase in the solvent exposure.

The solvent exposure of hydrophobic side-chains belonging to a sequence of five consecutive residues in the β-hairpin defines a possible starting point for the onset of the aggregation mechanisms. Several different possible conformations of the initial starting aggregates were also investigated. These simulations show that while hydrophobic contacts are important to bring together different monomers with a β-hairpin like conformation, more specific interactions such as hydrogen-bonding and coulombic interactions, should be considered necessary to provide further stabilization and ordering to the nascent fibrillar aggregates, as shown in the case of small peptide models [28].

For Aβ(12–28) peptides the atomic picture of the detailed mechanism of the evolution from α to β, combined with the atomic picture of model oligomeric aggregates provided in this work, can be very useful for the design of new constrained sequences or new drug candidates.

References

[1] P. Harrison, H. Chan, S. Prusiner, F. Cohen, Conformational propagation with prion-like characteristics in a simple model of protein folding, Prot. Sci. 10 (2001) 819–835.
[2] J. Harper, S. Wong, C. Lieber, P. Lansbury, Observation of metastable a- *beta* amyloid protofibrils by atomic force microscopy, Chem. Biol. 4 (1997) 119–125.
[3] W. Asbury, S. Dickinson, K. Bailey, The X-ray interpretation of denaturation and the structure of the seed globulins, Biochem. J. 29 (1935) 2351.
[4] E. Eanes, G. Glenner, X-ray diffraction studies on amyloid filaments, J. Histochem. Cytochem. 16 (1968) 673–677.
[5] M. Blake, C. Blake, From the globular to the fibrous state: protein structure and structural conversion in amyloid formation, Q. Rev. Biophys. 31 (1998) 1–39.
[6] W. Jong, A. Lomakin, M. Kirkitadze, D. Teplow, S. Chen, G. Benedek, Structure determination of micelle-like intermediates in amyloid beta-protein fibril assembly by using small angle neutron scattering, PNAS 99 (2002) 150–154.
[7] D. Klimov, D. Thirumalai, Dissecting the assembly of A β(16–22) amyloid peptides into antiparallel beta sheets, Structure 11 (2003) 295–307.
[8] J. Straub, J. Guevara, S. Huo, J. Lee, Long time dynamic simulations: exploring the folding pathways of an Alzheimer's amyloid a beta-peptide, Acc. Chem. Res. 35 (2002) 473–481.
[9] J. Gsponer, U. Haberthuer, A. Caflisch, The role of side chain interactions in the early steps of aggregation: molecular dynamics simulations of an amyloid–forming peptide from yeast prion Sup35, Proc. Natl. Acad. Sci. U.S.A. 100 (2003) 5154–5159.
[10] B.Y. Ma, R. Nussinov, Stabilities and conformations of Alzheimer's beta-amyloid peptide oligomers (A β(16–22') A β(16–35) and A β(10–35)): sequence effects, Proc Natl. Acad. Sci. U.S.A. 99 (2002) 14126–14131.
[11] J.F. Flood, J.E. Morely, E. Roberts, Amnestetic effects in mice of four synthetic peptide homologous to amyloid β-protein in patients with Alzheimer's disease, Proc Natl. Acad. Sci. U.S.A. 88 (1991) 3363–3366.
[12] J.F. Flood, J.E. Morely, E. Roberts, An amyloid β-protein fragment, A β(12–28), equipotently impairs post-training memory processing

when injected into different limbic system structures, Brain Res. 663 (1994) 271–276.
[13] P.E. Fraser, J.T. Nguyen, W.K. Surewiez, D.A. Kirschner, Ph dependent structural transitions of Alzheimer's amyloid peptides, Biophys. J. 60 (1991) 1190–1201.
[14] P.E. Fraser, L. Levesque, D.R. McLachlan, Alzheimer's A β-amyloid forms an inhibitory neuronal substrate, J. Neurochem. 62 (1994) 1227–1230.
[15] T.G. Fletcher, D.A. Keire, The interaction of β-amyloid protein (12–28) with lipid environments, Prot. Sci. 6 (1997) 666–675.
[16] N. Guex, M.C. Peitsch, Swiss-model and the swiss-pdbviewer: an environment for comparative protein modeling, Electrophoresis 18 (1997) 2714–2723.
[17] H.J.C. Berendsen, J.P.M. Postma, W.F. van Gunsteren, A. Di Nola, J.R. Haak, Molecular dynamics with coupling to an external bath, J. Chem. Phys. 81 (1984) 3684.
[18] W.F. van Gunsteren, X. Daura, A.E. Mark, GROMOS force field, Encyclopedia Comput. Chem. 2 (1998) 1211–1216.
[19] W.F. van Gunsteren, S.R. Billeter, A.A. Eising, P.H. Hünenberger, P. Krüger, A.E. Mark, W.R.P. Scott, I.G. Tironi, Biomolecular Simulation: the GROMOS96 Manual and User Guide, vdf Hochschulverlag, ETH Zürich, Switzerland, 1996.
[20] H.J.C. Berendsen, J.R. Grigera, T.P. Straatsma, The missing term in effective pair potentials, J. Phys. Chem. 91 (1987) 6269–6271.
[21] B. Hess, H. Bekker, J.G.E.M. Fraaije, H.J.C. Berendsen, A linear constraint solver for molecular simulations, J. Comp. Chem. 18 (1997) 1463–1472.
[22] S. Miyamoto, P.A. Kollman, Settle: an analytical version of the shake and rattle algorithms for rigid water models, J. Comp. Chem. 13 (1992) 952–962.
[23] T. Darden, D. York, L. Pedersen, Particle mesh ewald. an n.log(n) method for ewald sums in large systems, J. Chem. Phys. 98 (1993) 10089–10092.
[24] D. van der Spoel, R. van Drunen, H. J. C. Berendsen, Groningen machine for chemical simulations, Department of Biophysical Chemistry, BIOSON Research Institute, Nijenborgh 4 NL-9717 AG Groningen (e-mail to gromacs@chem.rug.nl), 1994.
[25] R.A. Jarvis, E.A. Patrick, Clustering using a similarity measure based on shared near neighbors, IEEE Trans. Comp. 22 (1973) 1025–1034.
[26] G. Tiana, F. Simona, R.A. Broglia, G. Colombo, Thermodynamics of beta-amyloid fibril formation, J. Chem. Phys 120 (2004) 8307–8317.
[27] L.C. Serpell, C.C.F. Blake, P.E. Fraser, Molecular structur of a fibrillar Alzheimer's A β-fragment, Biochemistry 39 (2000) 13269–13275.
[28] M. Lopez de la Paz, K. Goldie, J. Zurdo, E. Lacroix, C.M. Dobson, A. Hoenger, L. Serrano, De novo designed peptide-based amyloid fibrils, Proc. Natl. Acad. Sci. U.S.A. 99 (25) (2002) 16052–16057.